Elastically Housed Kinematic Couplings for Interchangeable Electric Vehicle Batteries

by

Sarah A. Sams

Submitted to the Department of Mechanical Engineering
in partial fulfillment of the requirements for the degree of

BACHELOR OF SCIENCE IN MECHANICAL ENGINEERING

at the

MASSACHUSETTS INSTITUTE OF TECHNOLOGY

June 2024

Authored by:	Sarah A. Sams Department of Mechanical Engineering May 15, 2024
Certified by:	Alexander Slocum Professor of Mechanical Engineering, Thesis Supervisor
Accepted by:	Alexander Slocum Professor of Mechanical Engineering Precision Engineering Research Group

Elastically Housed Kinematic Couplings for Interchangeable Electric Vehicle Batteries

by

Sarah A. Sams

Submitted to the Department of Mechanical Engineering
on May 15, 2024 in partial fulfillment of the requirements for the degree of

BACHELOR OF SCIENCE IN MECHANICAL ENGINEERING

ABSTRACT

Commercial adoption of electric vehicle technologies has lagged due to immense charging downtime, but kinematic couplings have the potential to bridge this barrier by allowing for battery swaps and simultaneous operation and back-up battery charging. Designing parameters such as an elastic housing to damp the battery's connection could overcome challenges with regard to manufacturing tolerance and operational loads. Accounting for proper preload and compliance for disturbance rejection is critical to maintain sufficient electrical contact while avoiding arcing. Kinematic couplings can provide enough contact area through Hertz line contact for a low resistance electrical contact, and Hertz stresses under loads are reasonable for conductive materials to bear without yield for long life cycles. This paper explored kinematic couplings as electrical conductors for electric vehicles by modifying a 2002 GEM E825. Kinematic coupling modifications decrease charging downtime by 98.33%. Elastic housings for ball-socket Kinematic couplings are predicted to increase the hertz contact area by 2684%, while decreasing the stress factor by 98.9% from a typical ball-groove kinematic coupling of the same size, allowing for larger vehicle batteries operated under higher forces and currents. Elastically housed kinematic couplings are a promising design pathway towards interchangeable electric vehicle batteries.

Thesis supervisor: Alexander Slocum
Title: Professor of Mechanical Engineering

Acknowledgments

I'm deeply grateful to Aditya Mehrotra for supporting me, and to Professor Slocum for patiently taking on another senior bachelor thesis student. Special thanks to Mark Belanger for extraordinary machine-shop assistance; his expertise and insightful feedback were integral to the completion of this thesis.

Contents

List of Figures

Chapter 1

Introduction

Electric vehicles are becoming more prevalent among private consumers, but commercial vehicles represent the next opportunity to reduce emissions. Medium and heavy-duty trucks often used commercially represent 23% of the U.S.' transportation sector emissions—not even considering vehicles primarily for on-site agricultural or construction work [1]. Significant emission reduction necessitates electric vehicles target commercial consumers. The main barrier in commercial adoption for electric vehicles is extensive charging downtime as industry demands prolonged continuous operating time. Easily removable batteries would increase functional operating capacity for electric vehicles by enabling the simultaneous charging of backup batteries and vehicle operation, thereby minimizing operational interruption.

Several car companies have been pursuing proprietary battery swap systems. Prof. Slocum's Precision Engineering Research Group in the Dept. of Mechanical Engineering at MIT has been working on what might become a possible open design standard for rapid battery swap using a Kinematic coupling-based design to provide a robust solution to maintaining the contact repeatability and connection security required of a battery during vehicle operation. A kinematic coupling also allows for the combination of the battery's physical and electrical contacts, reducing the total number of connections, potential for misalignment, and installation complexity.

Considering precision alignment isn't necessary for the battery's electrical connections as much as security, introducing elastically compliant housings or dampers for kinematic couplings could further reduce necessary manufacturing tolerances while increasing design robustness in the face of high operational forces. An interchangeable battery interface must allow for competitively low changing times when compared with both current electric vehicle standards and the time required to fill a traditional gas tank, meaning that it must be possible to completely swap the battery below the 8-20 minutes necessary to fill a large vehicle with gas [2]. In addition, the material of the kinematic coupling needs to have low contact resistance and high thermal conduction to withstand high operating voltages. The design of the coupling must also be resistant to pollutant particles that would increase the electrical contact resistance as many commercial vehicles work in conditions filled with water, dust, or other contaminants.

The primary goal of this research is to explore the design considerations of an electrically conductive kinematic coupling for application to electric vehicles and improve robustness through elasticity. Modifying an electric 2002 GEM E825's battery connection system, a vehicle often used by golf courses and groundskeeping companies, into a single kinetic coupling connector for operational testing enables concept verification. The battery selected for study is a 48V 105Ah Lithium LiFePO4 Battery. Further exploration of potential problems such as necessary preload, strain tolerance, thermal conductivity, electrical arcing, and pollutant particles are explored in this study. For this exclusively-electric vehicle, a competitive battery swap time is under the original battery's 9.4 hour charging time [3], but ideally would be near the 8-20 minutes necessary to fill a large vehicle with gas, as the swap time isn't expected to scale significantly with size. The kinematic coupling must also withstand horizontal forces from turns at vehicle's max acceleration, maintain thermal conduction at operating voltages of 48V without wear, have a contact resistance on the same order of magnitude as the internal vehicle's wires, and have a resistance to pollutant particles. A preload combined with the weight of the battery will allow the battery to maintain contact despite horizontal forces, and an elastic housing will compensate for both manufacturing tolerances and strains induced on the vehicle's frame by operating forces.

Chapter 2

Strategy and Concepts

A robust system for interchangeable electric vehicle batteries must physically support the system, maintain contact under operating disturbances, and properly relay an insulated electrical connection to the vehicle while remaining easy to swap. It must also not degrade significantly over an intended life cycle with exposure to common pollutants. Kinematic couplings (KC) represent a promising physical interface for the connection due to the ease of connection installation and high level of security. Elastic housings for kinematic couplings would drastically decrease the necessary level of manufacturing precision and increase the coupling's robustness under operating vibrations, loads, and deformations. To create a satisfactory electrical connection, the coupling must additionally maintain low contact resistances, reasonable operating temperatures, and avoid arcing.

2.1 Kinematic Couplings

Often used for precision machine design, kinematic couplings are exactly constrained mechanisms that can provide large stiffnesses, load capacities, and repeatability at relatively low manufacturing tolerances. Objects in free space have six degrees of freedom—colloquially known as forward/backward, up/down, left/right, yaw, pitch, and roll—and kinematic couplings impose six constraints to completely control the location of the coupling. Over-constraint requires high manufacturing tolerances to avoid extra stresses, while under-constraint can leave creations unstable. Consider designing a line as an example for over-constraint. Any two points allow a line to be produced between them, but for a third point to be included in the line, it must be precisely on the line. Similarly, if an item is under-constrained, it may end up as a two-legged stool and require precise balance to sit upon without tipping. Kinematic couplings adhere to exact constraint by creating six points of contact to control an object's six degrees of freedom [4]. Hertz contact theory is often leveraged by kinematic couplings to predict the high local stresses created between objects in point or line contact. Hertz contact stresses are frequently the cause of crack propagation, fragmentation, and fatigue failure in couplings. For a long-lasting kinematic coupling, Hertz contact stresses should not exceed 50% of the ultimate shear stress of the kinematic coupling material [4].

A common three-groove kinematic coupling is shown in figure 2.1. Small contact radii are common in kinematic couplings because it improves the repeatability of the kinematic

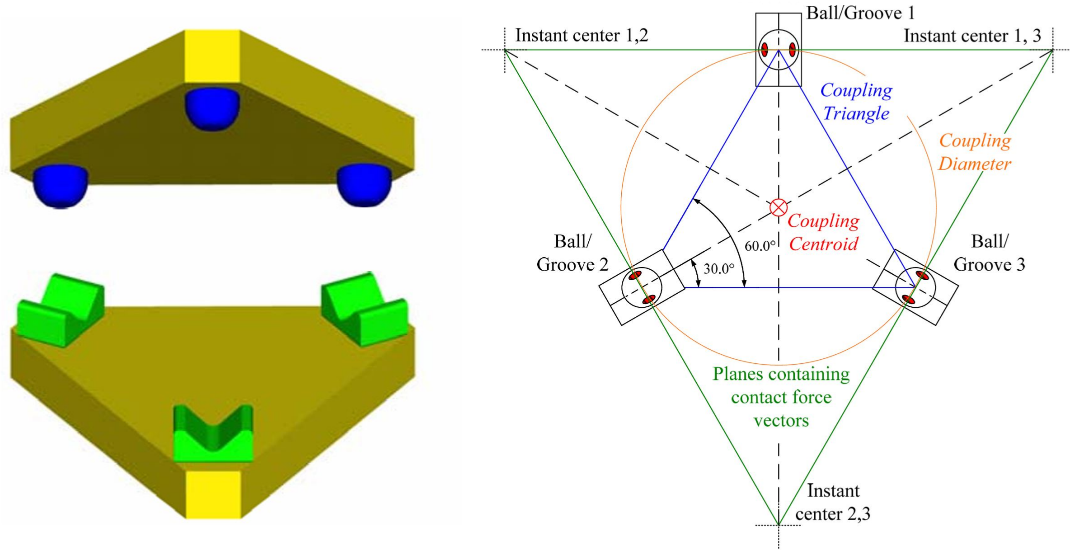

Figure 2.1: The generic geometry of ball and groove kinematic couplings is shown above to the left, and a diagram of their placement is shown on the right. Each ball and groove pair is spaced 120°apart around the coupling diameter to evenly distribute loading. The red ellipses represent the six contact points. The center of mass does not have to be aligned with the coupling centroid, but must be within the coupling triangle for stability [4].

coupling, specifically its precise location each use cycle. Historically kinematic couplings were used for precision and repeatability, making small contact radii desirable, however, it also increases Hertz stresses and limits loading. To adapt kinematic couplings for high-load, low-precision contact situations such as automotive electrical contacts, larger contact radii are preferable and additionally allow for lower electrical contact resistances. One such way to increase the load capacity of a kinematic coupling was dubbed the "canoe ball" by Alexander Slocum in 1986, wherein the contact region emulates a ball of much greater radius within the same size v-groove, thus significantly increasing the load capacity while maintaining an elliptical area of Hertz point contact [5]. Alternatively, as the electrical connection in an electric vehicle only needs to be secure, rather than precise, the over-constraint created by a larger contact radius can instead be negated by adding an additional degree of freedom, creating a quasi-kinematic coupling. In this case, a sphere contacting a conical socket would maintain a much larger area of Hertz line contact, further increasing the loading capacity and allowing for a larger preload to increase contact security despite on-road disturbances.

2.2 Vibration Isolator

A compliant mount or sleeve such as a vibration isolator for each of the vehicle frame's three conical grooves would add additional degrees of freedom to the system to prevent over-constraint while improving robustness against the conditions commonly experienced by vehicles. Even consumer road vehicles often experience large torques and low frequency disturbances during operation that can temporarily warp vehicle frames. Without compliance, these conditions could damage or disconnect a kinematic coupling's electrical connection by displacing the location of a groove. Compliant mounts could deform to maintain groove-ball contact despite system disturbances.

The ball and conical groove kinematic coupling is already relatively resistant to local torques and vertical displacements, as the ball and conical groove's connection is rotationally symmetric to accommodate for angular misalignment. However, the system needs compliance for horizontal displacement due to deformation of the vehicle's frame during operation. Extra compliance within the mount creates more movement of the battery while maintaining electrical contact, but too little compliance stresses the system, therefore the mounting system should aim for extra compliance.

Estimating the stresses observed in the vehicle during operation to find expected displacements would be tedious when the vehicle's frame has already been engineered to withstand the expected conditions with a hefty safety factor. Thus, a compliant mount should be able to tolerate the max horizontal displacement the vehicle frame can elastically accommodate before yielding, therefore ensuring that the vehicle would fail before the battery connection. The compliant mount's natural frequency under loading should also fall beyond the expected range of disturbance frequencies for vehicles, generally between 15-300Hz [6]. Conveniently, compliant materials such as plastics and rubbers that are often used as dampers also may act as electrical insulators for the kinematic coupling's electrical contact.

2.3 Electrical Considerations

To ensure the kinematic coupling is not only a suitable physical contact for the battery-vehicle interface, but also an electrical one, it must maintain an electrically insulated connection between the battery and vehicle and a negligible contact resistance. Considerations include surface corrosion, thermal conductance, arcing, and pollutants such as dust, debris, or water contamination.

The kinematic coupling must not only act as an interface for positive and negative electrical contacts on more complex vehicles, but also send varying control and feedback signals. To accomplish this, the ball and cone kinematic couplings can be segmented with insulators between each contact, however extensive research into signal interference would be necessary.

The kinematic coupling must be made of a conductive material, such as copper, that is able to withstand the maximum Hertz contact stresses that occur internally, below the contact surfaces. However, conductive materials often degrade under operating conditions due to humidity or oxidization. At 100 °C, Copper oxide film grows 2nm every 9 seconds, which greatly increases contact resistance over time [7]. Plating the kinematic coupling is necessary to resist corrosion and film development that could increase the coupling's contact resistance. Because maximum Hertz stresses occur beneath the contact surface, a layer of plating (industrially between 250-760 nanometers thick), won't affect the kinematic coupling's yield stress [7].

The kinematic coupling must be thermally conductive enough to ensure power dissipation due to internal resistance at operating voltages to avoid heating the kinematic coupling beyond electric insulation's max operating temperature. At higher voltages, contact welding would also be a concern, but the electrical insulation would fail before a contact weld occurs.

At higher voltages, a cooling system may be necessary.

Electrical arcing occurs when a voltage difference reaches the breakdown voltage of a material or gas and is roughly proportional to the product of the material's length, and, in the case of a gas, pressure [8]. However, Paschen's law is a more accurate relationship between the breakdown voltage of a gas, pressure, and arc distance that shows that the minimum breakdown voltage at one atmospheric pressure is 327 volts at 7.5 micrometers [9]. This minimum occurs because at smaller distances there are not enough ionizing collisions in the gap distance to carry an arcing current [10]. If the vehicle's operating voltages at atmospheric pressure are below 327 volts, arcing will not occur despite the curvature of the kinematic coupling's components, nor the gap distance caused by surface irregularities as long as the two surfaces maintain contact. Nevertheless, durable electric insulation still requires that the isolator's dielectric voltage breakdown is 3x as large as the system's predicted operating standards even at max displacements [7].

A bellows boot surrounding each of the three ball and cone joints would improve pollutant resistance in a cost-effective manner, significantly decreasing the number of contaminants introduced during operation. Eventually, a more sophisticated system such as pressurized air would be desired to limit pollutants during battery installation and removal, as commercial vehicles are often operated in dusty or moist environments. A bellows boot must tolerate the displacement induced by battery installation, as well as avoid restriction of the elastic vibration isolator's deformation.

2.4 Design Sketches

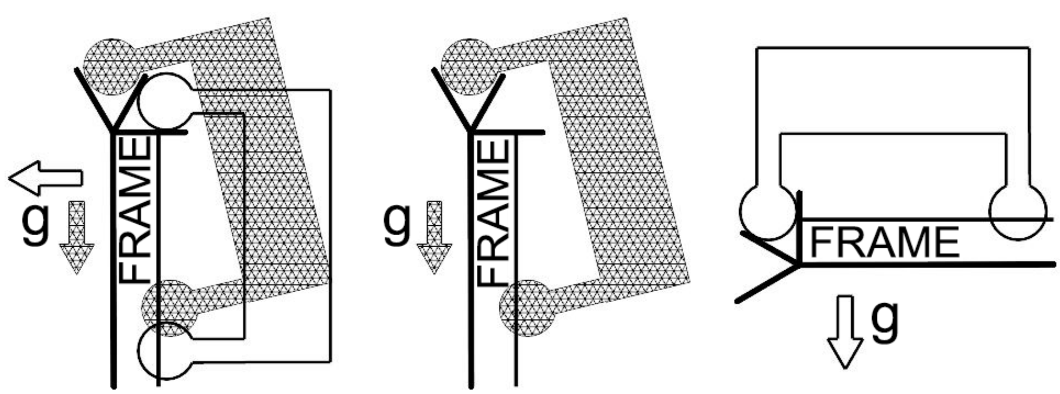

Figure 2.2: The diagram above shows two potential configurations of the same standard battery mounting interface. The shaded battery is mounted vertically, while the non-shaded is horizontal.

A spherical ball in a socket not only provides increased capability for preload but could also allow for a bidirectional mount in which varying vehicles could horizontally or vertically constrain the same standard battery interface, as depicted in figure 2.2.

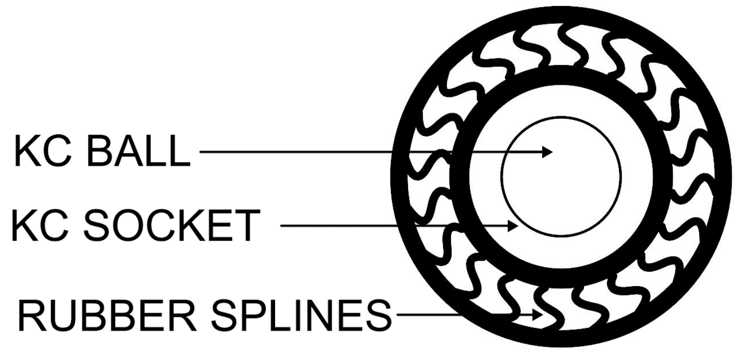

Figure 2.3: A rubber wheel with spokes could be created with specific compliance as the incompressible rubber deforms under loading.

A wheel of rubber with spokes inlaid with the KC socket as seen in figure 2.3 would allow for deflection to compensate for the over-constrained spherical socket coupling while electrically isolating the coupling and improving resistance to vibration. Curved splines provide additional stiffness against torsional forces but may not be necessary. This compliance could also be for manufacturing tolerances and vehicle frame deformation. A potential assembly is shown in figure 2.4. Magnetic switchable devices offer a promising application of preload without substantially increasing assembly weight or swap time.

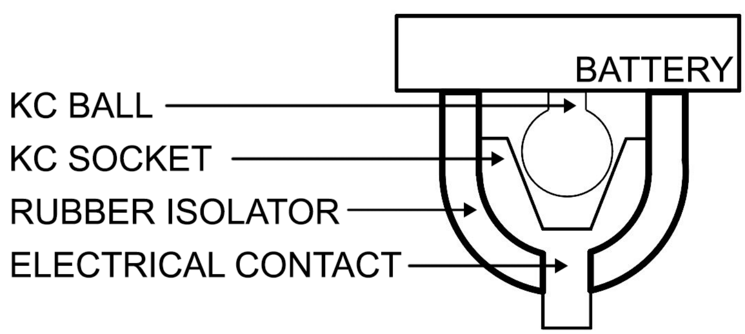

Figure 2.4: The generic ball and spherical socket layout as shown above would provide compliance and electrical isolation for the system

Chapter 3

Analysis and Theory

3.1 Preload Calculations

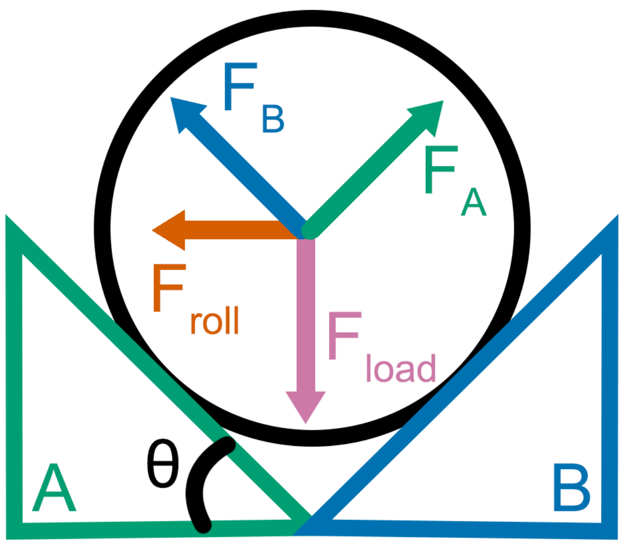

Figure 3.1: A force-body diagram for the ball and socket KC groove is pictured above. F_{load} is the force of preload, F_{roll} is the centripetal force as the car turns, θ is the angle of the cup's slope, F_A is the normal force from wall A, while F_B is the normal force from wall B.

Applying the right amount of preload to the battery is essential to ensure the kinematic coupling stays secure even as the vehicle accelerates and experiences vibrations or other disturbances during operation. The maximum force the coupling should experience is F_{roll}, the centripetal force as the car turns at maximum load m, maximum acceleration a, and minimum turn radius r.

$$F_{roll} = \frac{ma^2}{r}$$

F_{roll} must be less than the x-component of the normal force from wall A, F_{AX}, minus the x-component of the normal force of wall B, F_{BX}, to remain stationary. The F_{load} must also be equal to the sum of F_{AY} and F_{BY}.

$$F_{roll} < F_{AX} - F_{BX}$$

$$F_{load} = F_{AY} + F_{BY}$$

Geometric relationships between F_A, F_B, F_{AX}, F_{BX}, F_{AY}, and F_{BY} are given by the six equations listed below. The ball and socket are both curved surfaces, but theta is approximated as 45 °because the contact surfaces are tangent to one another at the contact point.

$$F_B^2 = F_{BX}^2 + F_{BY}^2$$

$$F_A^2 = F_{AX}^2 + F_{AY}^2$$

$$F_{AX} = F_A * cos(\theta)$$

$$F_{AY} = F_A * sin(\theta)$$

$$F_{BX} = F_B * cos(\theta)$$

$$F_{BY} = F_B * sin(\theta)$$

Matlab code is given in appendix A to solve for the necessary preload given θ, m, a, and r. The force of roll is divided by 3 for each of the three ball-cup pairs, and the preload is given for each ball-cup pair, so the total preload is 3X the given Matlab value for F_{load}.

3.2 Hertz Contact

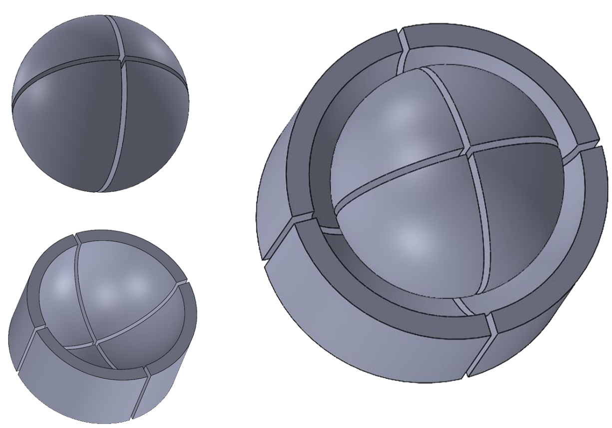

Figure 3.2: A ball and socket pair for the kinematic coupling is pictured above. Segmented into fourths, the pair could potentially transmit four separate signals with steps taken to explore proper signal isolation

The hertz line contact for the ball and socket design will be found assuming the radius of the socket is 1.2x larger than that of the ball, with contact occurring 45° from vertical. The same equations for two cylinders can be modified for the sphere and socket. The socket's concave diameter will be taken as negative, while the ball's convex diameter will be positive. The length of contact will be the sphere's circumference at 45°. If calculating for a segmented sphere, subtract the width of the gaps.

$$L = \pi d_{ball} cos(\theta)$$

The load applied to the contact is component normal to the 45° contact surface between the sphere and socket.

$$F_{Hertz} = \frac{F_{Preload}}{cos(\theta)}$$

The equivalent elastic modulus of contact is given below in terms of the Young's modulus of elasticity and Poisson's ratio of the ball and socket's materials:

$$E_{eq} = \frac{1}{\frac{1-\nu_{ball}^2}{E_{ball}} + \frac{1-\nu_{socket}^2}{E_{socket}}}$$

Keeping in mind that d_{socket} is both negative due to curvature, and slightly larger than d_{ball}, The width of the hertz contact can be found:

$$W = 2 * \sqrt{\frac{2F_{Hertz} d_{ball} d_{socket}}{\pi L E_{eq}(d_{ball} + d_{socket})}}$$

The contact pressure can now be calculated:

$$P_{hertz} = \frac{2 * F_{Hertz}}{\pi L \frac{W}{2}}$$

The maximum shear stress for hertz line contact is always $0.3P_{hertz}$ and occurs at $0.786\frac{W}{2}$ below the surface [11]. The resulting stress factor should be less than 0.5 for a long part lifetime, and can be determined:

$$\sigma_{SCF} = \frac{0.3P_{hertz}}{\frac{\sigma_{UTS}}{2}}$$

Surface roughness induces small contact widths, but as the couplings wear over use cycles, this effect may be neglected over time. However, induced contact width may be calculated:

$$W_{ind} = 8R\frac{d_{ball}}{2}$$

3.2.1 Hertz Ball-Groove vs Ball-Socket

Hertz calculations are used for a brass ball of 1" in diameter to compare the contact area and load capacities for ball-groove KC's and ball-socket KC's.

It's predicted that the ball-groove design induces a contact surface of 1.9 mm^2, while the ball-socket design induces a contact surface of 52.9 mm^2.

The ball-socket design increases Hertz contact area by 2684% when compared with a ball-groove design's point contact, significantly decreasing electrical contact resistances.

Additionally, the predicted stress factor in a ball-groove design is 6.37, while the stress factor in a ball-socket design is 0.07. This demonstrates a 98.9% decrease in stress factor, and allows for the conductive, soft brass to have a long part lifetime despite the large preloads necessary.

3.3 Predicted Deformation

The local deformation of the vehicle frame underneath the battery can be overestimated by beam bending at yield, as car manufacturers have already designed car frames not to bend beyond the elastic regimen for anticipated conditions, and a car frame's shape is much stiffer than a beam. Using beam bending models, the maximum displacement can be calculated:

$$\delta_{Max} = \frac{5L\sigma_{yield}}{E_{frame}}$$

A quick, informal proof is shown in appendix B

3.4 Predicted Displacements

Each vibration isolator must be able to displace by some amount δ, which is equal to the manufacturing tolerance on the placement of each KC ball and socket plus the maximum amount of displacement due to distortion of the vehicle frame spread across the three vibration isolators. Each isolator will displace the same amount to accommodate any one isolator's displacement because it occupies the lowest energy configuration. Approximating the vibration isolator as a spring, the energy stored is equal to $E = \frac{1}{2}kx^2$. The energy configuration if one isolator displaces the distance is $E = \frac{1}{2}k(\delta)^2$, which is greater than if three isolators each displace 1/3 the distance: $E = \frac{1}{2}k((\frac{\delta}{3})^2 + (\frac{\delta}{3})^2 + (\frac{\delta}{3})^2) = \frac{1}{2}k(\frac{\delta^2}{3})$.

Because each vibration isolator displaces the same distance, the total amount they must each displace can be found by the difference in radii of their deformed cup's coupling diameter and the ball's coupling diameter. It is assumed that only the cups' coupling radius deforms as they are connected to the vehicle frame, while the balls are connected to the battery, which will ideally be isolated from any deformation. Initially, the coupling diameters, R_{ball} and R_{cup}, are equivalent (manufacturing tolerances may be assumed with displacements for ease of calculation). Assuming the initial coupling centroids are (0,0) and considering each of the balls and cups as points, the equation of the circle that defines the initial, un-deformed coupling diameter is:

$$R_{ball}^2 = x^2 + y^2$$

Assuming the worst, if each ball moves the maximum predicted displacement δ radially, the new, deformed location of each socket is:

$$(x + \delta sin(45), y + \delta sin(45))$$

The new center of the coupling diameter and deformed radius for irregular displacements can be found with linear algebra (see appendix C for details on using Microsoft Excel), however, as the max displacement of each coupling can be estimated to be approximately the same, each coupling must be able to accommodate its own max displacement.

Chapter 4

Design & Testing

4.1 Vehicle Modifications & Ball-Groove Adaptation

To begin testing kinematic couplings as battery connectors for electric vehicles, the GEM was modified to run on one 48V battery, and a traditional ball-groove coupling was used to prove the concept, and then the ball and socket design was implemented and iterated upon to better withstand expected operational conditions.

An electric 2002 GEM E825's battery connection system was modified to connect to a singular 48V 105Ah Lithium LiFePO4 Battery instead of six 12V deep-cycle batteries (see appendix D for wiring).

A two-part steel frame constructed from hollow stock 1" steel beams was used to support the battery on the back of the GEM, detailed measurements shown in figure 4.1. Steel ball-groove kinematic couplings were then attached to the frame, using 1" delrin for electrical isolation, and the KC's were electrically connected to the battery and GEM.

4.1.1 Ball-Groove Operation

The GEM electrically connected by steel ball-groove kinematic couplings was fully operational. Swapping the battery onto the new frame takes under five minutes, while the battery's complete charging time takes five hours, effectively decreasing downtime by 98.33%. Driven around for approximately half an hour, it experienced no thermal conductivity issues nor decreases in performance, therefore materials more conductive than steel–such as brass or aluminum–should also operate smoothly. However, upon disassembly, it was found that some arcing occurred on the couplings due to a lack of sufficient preload, shown in figure 4.3. The ratchet strap was used as a temporary preload device despite insufficient forces as a means for preliminary testing. Based on the calculations in chapter 2, a total preload of 1,350lbs is needed to ensure the KC's maintain contact. Preload application through magnetic switchable devices proves promising, functionally improving preload without significantly increasing the assembly's weight nor swap time.

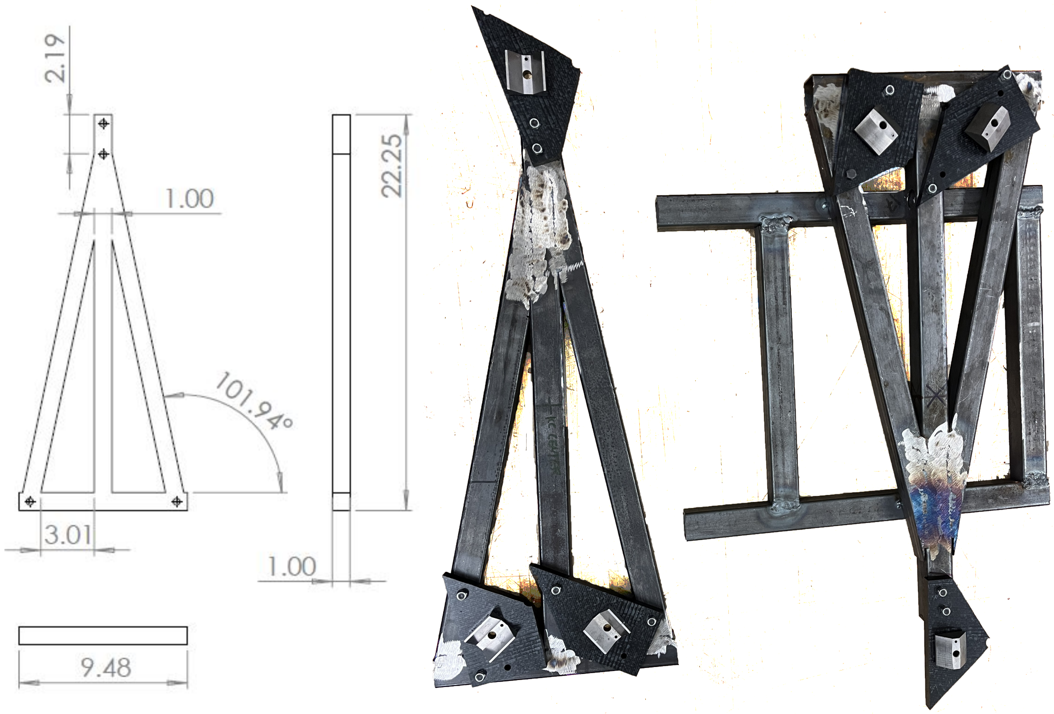

Figure 4.1: Above are custom welded steel frames to attach the kinematic coupling to the GEM. Steel ball-groove kinematic couplings are used as a proof of concept. Delrin scraps are used to electrically isolate the kinematic couplings from the steel frame. One pair of kinematic couplings are used for the battery's positive terminal connection, and the other the negative. The upper contacts are connected to a bolt used to electrically connect the battery, while the lower contacts use a bolt to connect to the GEM.

Figure 4.2: Above, the modified GEM with ball-groove KC's acting as physical and electrical connections is shown in operation. The battery is on the welded frame at the back of the vehicle. An orange ratchet strap applies preload to the system.

Figure 4.3: One of the KC's from the operated frame is shown above with the damage caused by arcing. Arcing occurred during vehicle operation because an insufficient preload allowed the couplings to separate as the vehicle drove over road irregularities.

4.2 Elastically-Housed Ball-Socket

After demonstrating that kinematic couplings can act as viable electrical connections for vehicles, dampers were added to improve contact robustness in the face of vibration and frame warping during operation. According to the calculations in chapter 2, if each coupling is able to deform 0.15" horizontally, they should be able to maintain contact despite any potential deformation of the GEM's aluminum frame, along with a manufacturing tolerance of ± 2 mm on each coupling pair. To minimize in-house manufacturing, an assembly (shown in Appendix E) was manufactured using brass and aluminum stock and off-the-shelf dampers with a maximum shear deflection of 0.2". The completed assembly is shown in figure 4.4. Two dampers are used in series for each coupling pair, thereby doubling the maximum shear deflection to 0.4", significantly more than required.

4.2.1 Vibration Damper Operation

The battery was not electrically tested as, when secured to the frame assembly, it caused the dampers to buckle under loading, shown in figure 4.5. The dampers were designed in the assembly under the assumption they would maintain horizontal planes under loading, which was not the case.

The damper's shear deflection is rated for <0.2", but this assumes that the damper's contacts are planes, thus preventing angular tilts that lead to bending, i.e. putting the ball's center of mass past its base. The ball-cup coupling that provides angular freedom causes the dampers to bend, translating the ball up to 1" horizontally under the battery's 100lbs force. Even if the coupling alignment were perfect, a slight turn would destabilize the system to

Figure 4.4: The finished damper ball and socket assembly is pictured above, with a flat plate of 1/16" thick aluminum ($R \leq 0.005\Omega$) used to complete the electrical connections from the sockets to the GEM. The battery is not pictured for clarity, but would rest on top of the assembly and similarly use aluminum to create an electrical connection with the KC balls.

failure.

The bending is also more sensitive to horizontal force disturbance with higher vertical preloads. The vehicle frame is angled slightly outwards, which is realistic as vehicles go up slopes, but contributes to the destabilized resting position. The added height of the dampers and the extra-long cups also exacerbates the problem by adding in larger moments, but even shortening the 1.5" cups down to the minimum 0.75", it would still be too unstable to drive.

Geometrically constraining the maximum deflection with a rigid pipe around each damper-coupling set, or a larger box with bumpers for the battery to sit within could potentially save the design, but it would still be precarious. Shorter, slightly harder dampers are available for purchase that would still meet the deflection requirements, but again, wouldn't fix the fundamental design constraint flaw: dampers are built to be connected to a plane for shear stress.

Regardless, elastic cup-ball KC's still have design promise with rubber over-molded spoke-dampers for strictly horizontal deflection, as the assumption that the rubber is constrained to a plane would be true, but the traditional form-factor shear damper of practical durometers or heights would not be sufficiently effective.

4.2.2 Ball-Socket Rubber Isolator

Initially, over-molded spoke-dampers akin to figure 2.3 were desired to create horizontal planar deflection, however, with the time given, professor Slocum suggested the design shown in figure 4.6, which was then adapted into figure 4.7. The parts from the initial off-the-shelf damper design were adapted according to the design specifications shown in appendix F

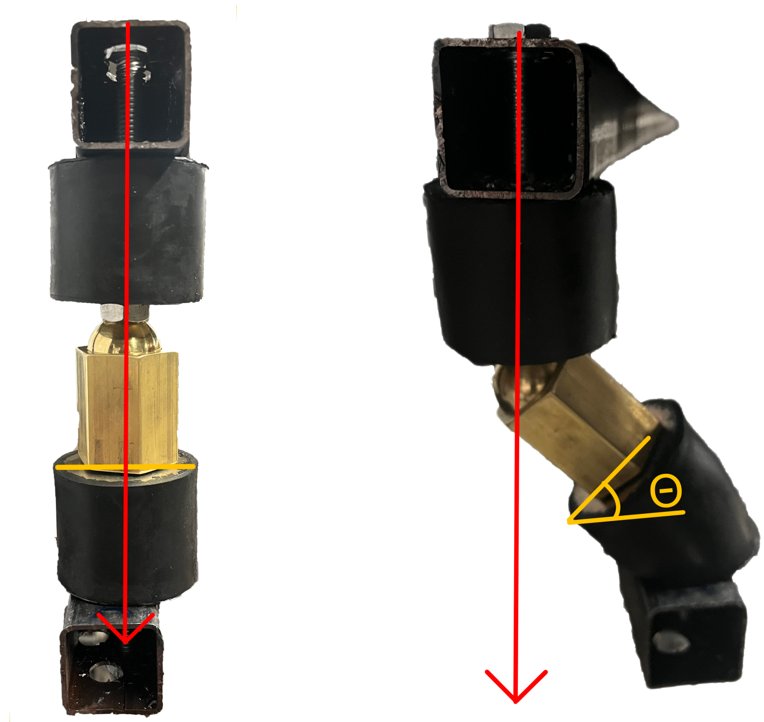

Figure 4.5: On the left is an unloaded configuration of the damper assembly, and on the right a load of 100lbs is applied to the assembly. The red line represents the translation of force throughout the structure, while the yellow line shows the angular displacement of the damper's surface. Under loading, the force creates a tipping moment by translating beyond the isolator's base, thus creating instability.

with 1/8" thick 30A durometer sheet rubber for damping and electrical isolation. The new design ensures that force is transferred at 45° into the isolator as shown in figure 4.7. This balanced force transfer minimizes the creation of moments. The final machined parts can be seen in figure 4.8.

4.2.3 Rubber Isolator Operation

The sheet rubber isolator assembly is more robust against disturbances than the vibration damper assembly, and was tested in a Texture Analyzer with a TA-25 probe at forces up to 500 N to determine the spring constant of a coupling pair. The spring constant of the assembly was found to be $189.2 \pm 0.3 \, \frac{N}{mm}$. Force-distances curves are shown in figure 4.9.

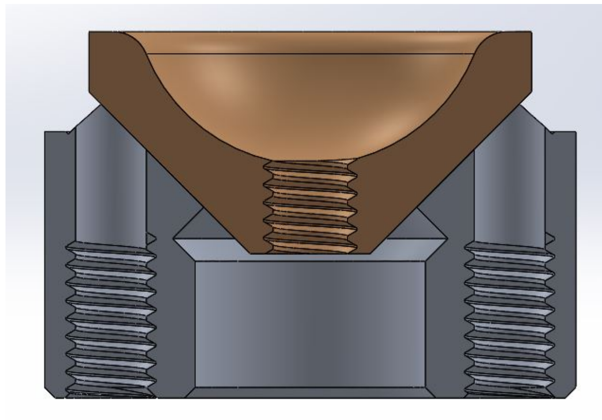

Figure 4.6: This design was suggested by prof. Slocum as an alternative solution to damper bending.

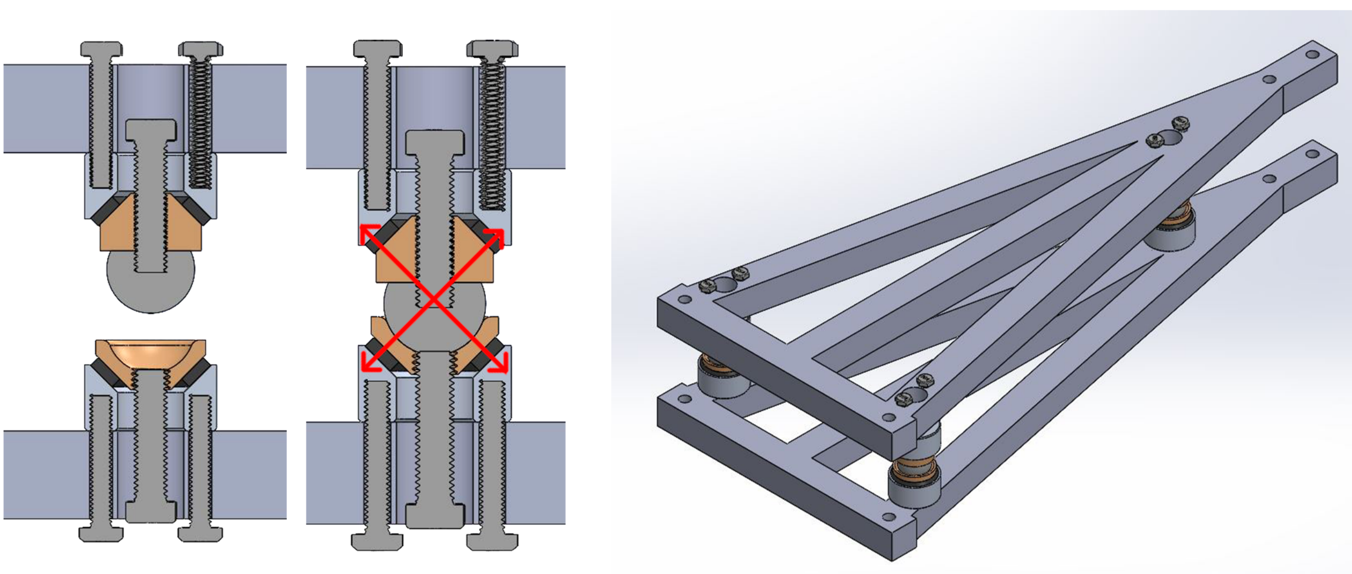

Figure 4.7: This design was adapted from the suggestion by prof. Slocum in figure 4.6. The red lines represent the force translation from the upper frame into the lower. The gold is brass, the black is rubber, and the gray is steel or aluminum.

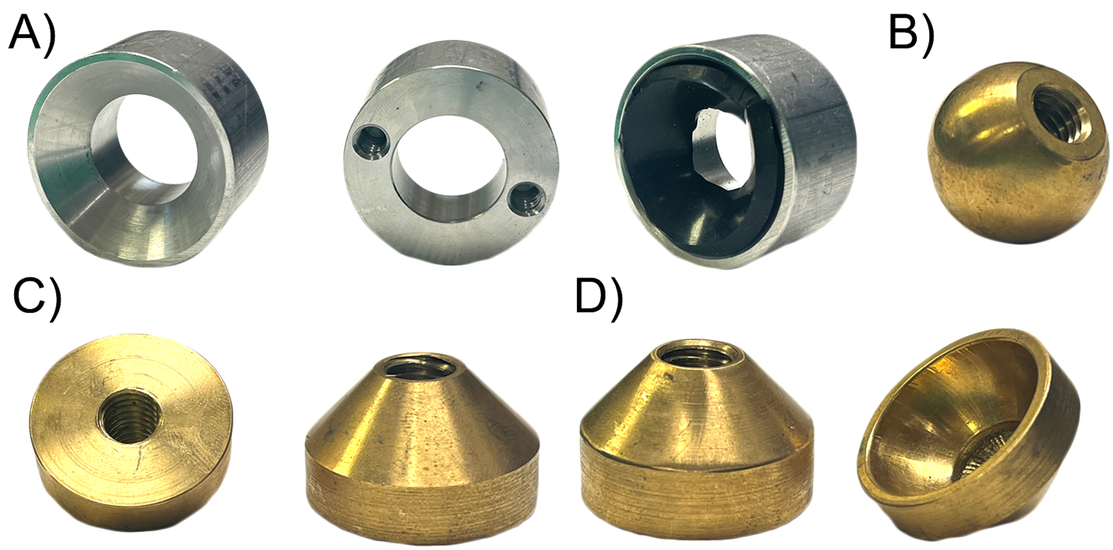

Figure 4.8: These parts were made from the design specifications in appendix F. Enough parts for three complete coupling pairs were made, but shown above from varying angles are A) one aluminum outer casing shown with and without rubber insert, B) one faced ball mount, C) a filled socket, and D) a socket.

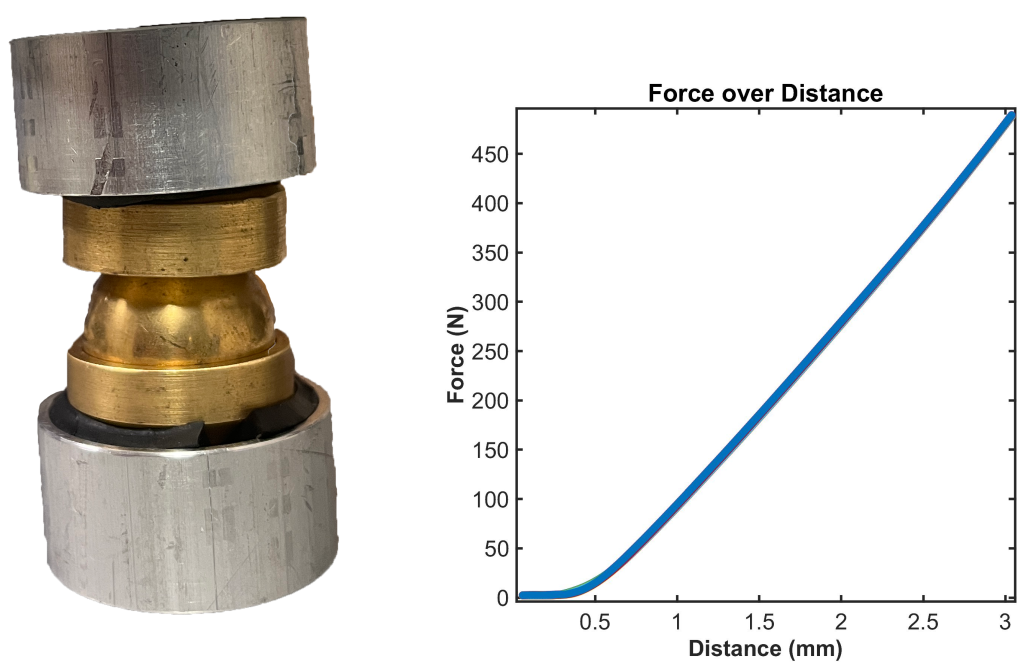

Figure 4.9: A coupling pair of the sheet isolator assembly is shown left, while ten trials of compression are overlaid on the graph to the right. The spring constant of the coupling was found to be $189.2 \pm 0.3\ \frac{N}{mm}$.

Chapter 5

Conclusion

Adapting electric vehicles for commercial and industrial use is an important step towards reducing global emissions. Elastically-housed kinematic couplings are a promising design pathway towards overcoming charging downtime by enabling time-efficient battery swaps. Key factors to consider when designing a kinematic coupling for electric vehicles include necessary preload to prevent coupling separation and arcing, an understanding of Hertz contact for coupling sizes and part lifetimes, electrical conduction and isolation, and tolerances for vehicle frame deformation under operation. Providing an elastic housing for electrical kinematic couplings could improve connections' contact robustness by enabling higher preloads, providing vibration isolation, and higher tolerances for vehicle frame warping. However, as demonstrated by the modified 2002 GEM E825's unhindered performance, steel kinematic couplings themselves are a viable electrical interface for electric vehicle battery connections that significantly increases functional operating capacity. A steel ball-groove kinematic coupling interface effectively decreased the 2002 GEM E825's charging downtime by 98.33% without hindering performance. Elastically housed ball-socket couplings are additionally predicted to increase the hertz contact area by 2684% while decreasing the stress factor by 98.9% from ball-groove couplings. This substantially improves part lifetimes and decreases electrical surface contact resistances. Further exploration into kinematic coupling designs and more efficient preload methods such as magnetic switchable devices have the potential to further decrease charging downtime even on large industrial vehicles.

Appendix A

Code listing

```
Theta = pi/4;

m = 453.696;
a = 1.2;
r = 5.3;

F_roll = ((m*a^2)/r)/3;

eq1  =   @(x)   x(4)^2 + x(5)^2 - x(3)^2    ;
eq2  =   @(x)   x(6)^2 + x(7)^2 - x(2)^2    ;

eq3  =   @(x)   x(1) - x(5) - x(7)          ;

eq4  =   @(x)   x(2) * cos(pi/4) - x(6)     ;
eq5  =   @(x)   x(2) * sin(pi/4) - x(7)     ;

eq6  =   @(x)   x(3) * cos(pi/4) - x(4)     ;
eq7  =   @(x)   x(3) * sin(pi/4) - x(5)     ;

eq8 =   @(x)   x(6) - x(4) - F_roll         ;

A = fsolve( @(y) [eq1(y); eq2(y); eq3(y); eq4(y); eq5(y); eq6(y); eq7
    (y); eq8(y)], ...
     [6000, 2000, 2000, 500, 500, 500, 500]);

F_load  = A(1);
F_A     = A(2);
F_B     = A(3);
F_BX    = A(4);
F_BY    = A(5);
F_AX    = A(6);
F_AY    = A(7);
```

Appendix B

Deflection Derivation

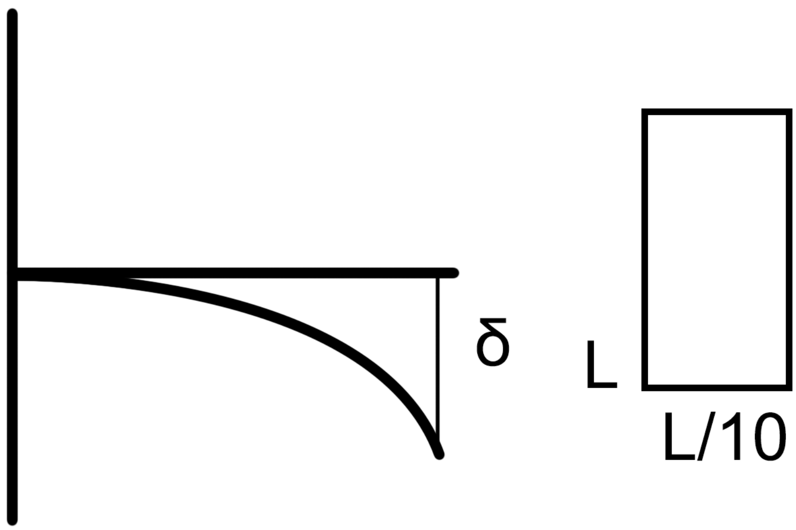

Note that $\sigma_Y = \frac{ML}{10I}$ and $\delta = \frac{ML^2}{2EI}$

$$M = \frac{10\sigma_Y I}{L}$$

$$\delta = \frac{\frac{10\sigma_Y I}{L} L^2}{2EI}$$

$$\delta = \frac{\sigma_Y L}{5E}$$

Appendix C

Excel Radii Subtraction

–	A	B
1	X_1	Y_1
2	X_2	Y_2
3	X_3	Y_3
4	$Center_X$	$Center_Y$
5	–	Radius

$$Center_X = \text{TRANSPOSE(MMULT(MINVERSE(2*(A2:B3-A1:B1)),MMULT(A2:B3}\wedge 2 - A1 : B1 \wedge 2, 1; 1)))$$

$$Radius = SQRT(SUMPRODUCT((A1 : B1 - A4 : B4) \wedge 2))$$

Appendix D

GEM Modified Wiring Diagram

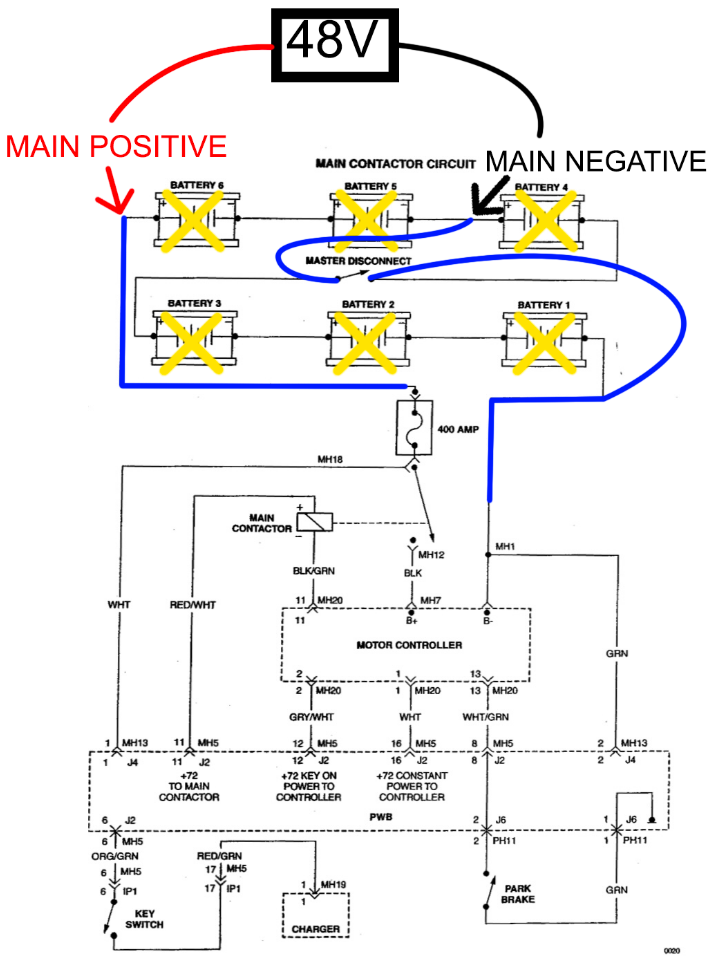

The GEM's modified electrical diagram, to allow one 48V battery instead of six 12V batteries, is shown above. The new circuit is shown in blue and the main 48V battery's connections' are shown in red for positive and black for negative [12]. Batteries 5 and 6 are underneath the vehicle's hood, while 1-4 and the master disconnect are underneath the vehicle's seat, with battery 1 located closest to driver's side. To convert the system, battery 1's negative was disconnected and wired to the master disconnect, then battery 4's positive was disconnected and wired to the master disconnect. Next, battery 5's main negative was disconnected and connected to the 48V's negative terminal. Battery 6's positive was disconnected and wired to the 48V's positive terminal.

Appendix E

Damper Assembly

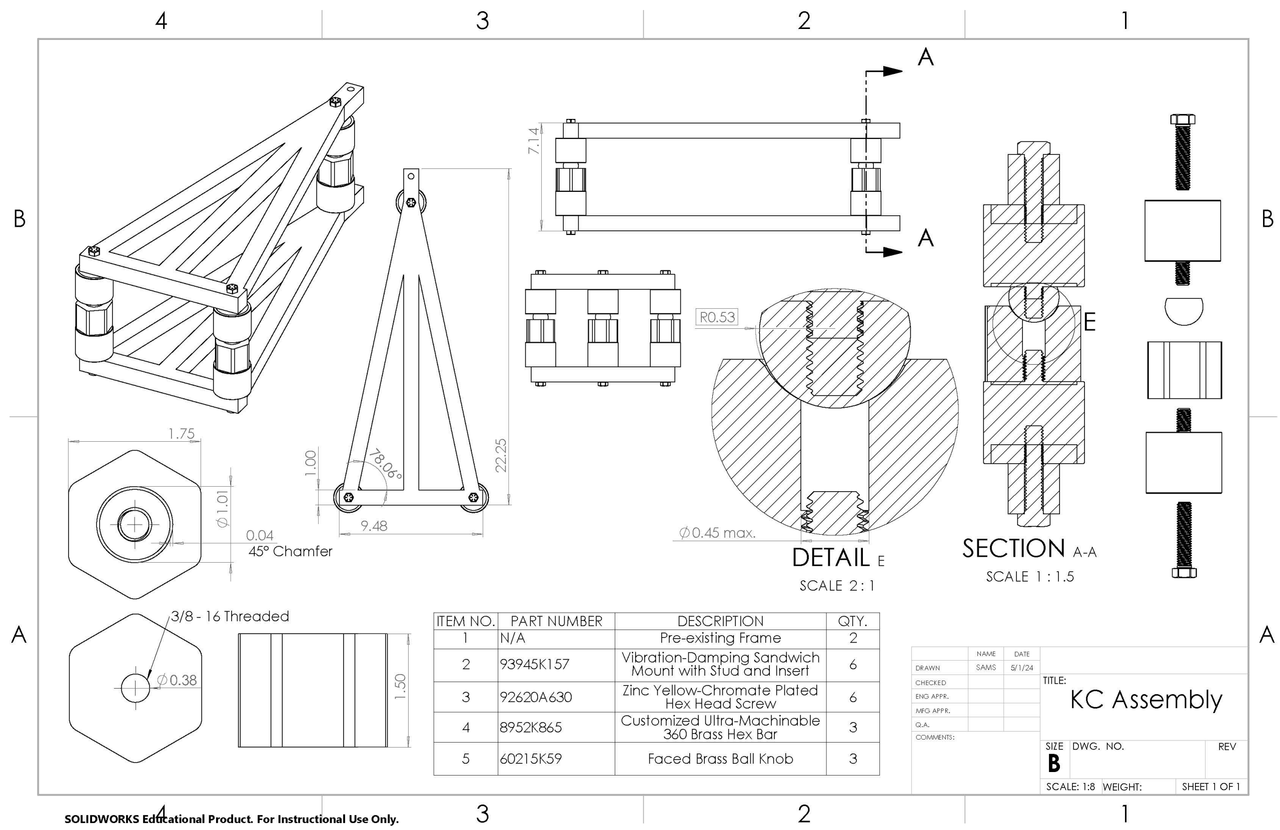

ITEM NO.	PART NUMBER	DESCRIPTION	QTY.
1	N/A	Pre-existing Frame	2
2	93945K157	Vibration-Damping Sandwich Mount with Stud and Insert	6
3	92620A630	Zinc Yellow-Chromate Plated Hex Head Screw	6
4	8952K865	Customized Ultra-Machinable 360 Brass Hex Bar	3
5	60215K59	Faced Brass Ball Knob	3

The brass balls are faced to ensure an adequate electrical contact surface, and the edges of the socket are chamfered to eliminate the potential for edge loading. A ball end mill is used to create the socket holes. Electrical contact surfaces are polished to improve resistances.

Appendix F

Rubber Assembly

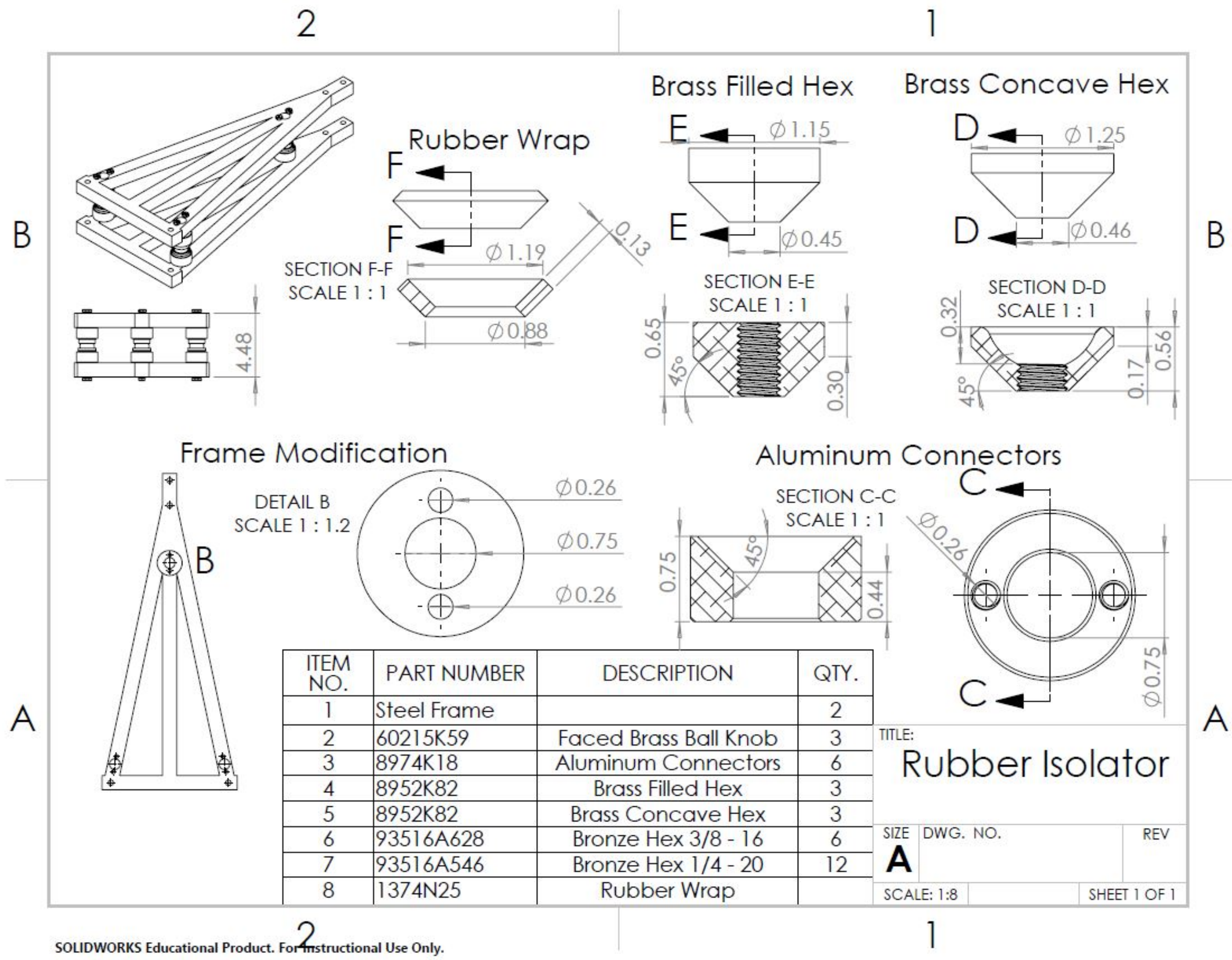

ITEM NO.	PART NUMBER	DESCRIPTION	QTY.
1	Steel Frame		2
2	60215K59	Faced Brass Ball Knob	3
3	8974K18	Aluminum Connectors	6
4	8952K82	Brass Filled Hex	3
5	8952K82	Brass Concave Hex	3
6	93516A628	Bronze Hex 3/8 - 16	6
7	93516A546	Bronze Hex 1/4 - 20	12
8	1374N25	Rubber Wrap	

The hex sockets from the damper assembly are split into two parts: one turned into the brass filled hex, and the other the brass concave hex. Aluminum stock is turned into six aluminum connectors. The frame is modified with new holes to connect to the aluminum. The center hole of the frame and aluminum connectors must be large enough for a hex socket. Rubber is cut into arcs and wrapped with adhesive onto the aluminum connectors.

References

[1] U. E. P. Agency. "Fast facts on transportation greenhouse gas emissions." (2021), URL: https://www.epa.gov/greenvehicles/fast-facts-transportation-greenhouse-gas-emissions.

[2] Joe. "How long does it take to fuel a semi truck?" (2021), URL: https://truckile.com/how-long-does-it-take-to-fuel-a-semi-truck/.

[3] *2002 global electric motorcars e825 2-passenger*, U.S. Department of Energy, Office of Transportation Technology, 3601 7th Avenue NW Fargo, ND 58102, 2002. URL: https://avt.inl.gov/sites/default/files/pdf/nev/gem2pass.pdf.

[4] A. Slocum, "Kinematic couplings: A review of design principles and applications," *International Journal of Machine Tools and Manufacture*, vol. 50, no. 4, pp. 310–327, 2010, Design of Ultraprecision and Micro Machine Tools and their Key Enabling Technologies, ISSN: 0890-6955. DOI: https://doi.org/10.1016/j.ijmachtools.2009.10.006. URL: https://www.sciencedirect.com/science/article/pii/S0890695509002090.

[5] P. Willoughby and P. John, "Kinematic alignment of precision robotic elements in factory environments," May 2005.

[6] T. J. Gordon and Z. Bareket, "Vibration transmission from road surface features – vehicle measurement and detection.," The University of Michigan Transportation Research Institute (UMTRI), 2901 Baxter Road, Ann Arbor, MI 48109-2150, Nissan Technical Center North America, Inc. Jan. 2007.

[7] P. G. S. (Editor), *Electrical Contacts: Principles and Applications*, 2nd ed. Boca Raton: Taylor and Francis Group, 2017. URL: https://www.taylorfrancis.com/books/edit/10.1201/b15640/electrical-contacts-paul-slade.

[8] C. L. Wadhwa, *High Voltage Engineering*, 2nd ed. New Age International Pvt Ltd, 2007, pp. 10–12. URL: https://books.google.com/books/about/High_Voltage_Engineering.html?id=4rQu1M0sjRAC.

[9] M. A. Lieberman and A. J. Lichtenberg, *Principles of Plasma Discharges and Materials Processing*, 2nd ed. Hoboken, N.J: Wiley-Interscience, 2005. URL: https://isbnsearch.org/isbn/9780471720010.

[10] J. B. Calvert. "Electrical discharges." (2005), URL: http://www.physics.csbsju.edu/tk/370/jcalvert/dischg.htm.html.

[11] A. Slocum. "Fundamentals of design." (2020), URL: https://meddevdesign.mit.edu/fundamentals-downloads/?eeFolder=FUNdaMentals-Chapters&eeListID=1&ee=1.

[12] *2001-2004 gem owners manual*, Global Electric Motorcars, LLC, 3601 7th Avenue NW Fargo, ND 58102, 2004. URL: https://manualzz.com/doc/6294687/2001-2004-gem-owners-manual.